# Carboxyl- and amine-functionalized carboranethiol SAMs on Au(111): A dispersion-corrected density functional theory study

Merve Yortanlı and Ersen Mete*
*Department of Physics, Balıkesir University, Balıkesir 10145, Turkey*

(Received 18 May 2020; revised 14 August 2020; accepted 8 September 2020; published 28 September 2020)

The morphological and electronic properties of isolated and monolayer phases of carboxyl- and amine-functionalized carboranethiols on unreconstructed Au(111) were determined using density functional theory calculations including van der Waals interactions. The groups are effective in the assembly of pristine adlayers on gold and also offer functionality when exposed at the SAM-environment interface. Anisotropy brought by both functional groups increases tilting of carboranethiols relative to the surface normal and absolute values of the dissociative chemisorption energies. Positional isomerization and the functional groups modify the molecular dipole moments which influence the adsorption characteristics. Even though carboxylic acid and amine groups have different chemical properties, they have similar effects on the adsorption characteristics of carboranethiols. Dense packing favors intermolecular interactions which gives a stronger binding relative to isolated adsorption. The carboranethiols with the functional groups can be arranged in the same lateral direction or in a dimer conformation with molecules facing each other. Carboxyl and amine groups offer functionalization of carboranethiol SAMs and in conjunction with positional isomerization shift tunability ranges of the work function of gold to higher energies.

DOI: 10.1103/PhysRevMaterials.4.095002

## I. INTRODUCTION

Thiol-based (R-S-H) self-assembled monolayers (SAM) are promising for applications in different fields such as molecular electronics, nanotechnology, surface wetting and molecular recognition [1–10]. The characteristics of SAMs are related to coated molecule on the surface as well as to the coating density. The molecular density of SAMs is effective in inter-molecular and molecule surface interactions and plays a crucial role in the film's structural and electronic properties. For instance, work function of metal electrodes used in the design of organic electronic devices can be modified by adjusting dipole moments of different thiol SAMs attached to those electrodes. Thiol SAMs provide a great advantage in many applications, and therefore, has been the subject of many experimental [11–30] and theoretical [31–41] studies. Moreover, additional functional groups were shown to be effective in modification of the work function of gold substrates. Lee *et al.* demonstrated the tunability of the work function by amine- and carboxylic acid-functionalized alkanethiol SAMs [20].

Dicarbacloso-dodecaborane thiol ($C_2B_{10}H_{12}S$, briefly will be called as carboranes or CT) derivatives are potential molecules for SAMs in various fields of applications. Due to their spherical stable nature, the dipole moment vectors and orientations can be easily modified by changing the position of the carbon atoms in the cage structure. This kind of material design gives the possibility to modulate the work function of the surface on which it is coated [12,13,15,19,21–24,27–29,42]. Lübben *et al.* modulated the work function of Ag(111) with pure and mixed SAM structures formed using 1,2- and 9,2-type carboranedithiol molecules [1,2-$(HS)_2$–1,2-$C_2B_{10}H_{10}$ and 9,12-$(HS)_2$–1,2-$C_2B_{10}H_{10}$] having opposite dipole orientations on the silver surface [21]. Kim *et al.* studied Au(111) with SAMs composed of 1,7 M1- and M9-type carboranes (1-HS-1,7-$C_2B_{10}H_{11}$ and 9-HS-1,7-$C_2B_{10}H_{11}$) [27]. They were able to systematically modulate the Au(111) work function in the 0.8 eV range with different coating ratios. When they transfer their coatings to OFET design, mixed SAM structures produced better yields. Also, the carboranes can be systematically functionalized with various ligand groups with different electronic properties [28]. In addition, functionalized carboranes alter the electronic structure of the surface on which they are attached. As a result, SAMs with functionalized carboranes gives opportunity to systematically change the electronic and the surface properties of materials.

Functionalized CT-SAMs have recently received an increased attention [28,43,44]. Ito *et al.* brought insights into surface chemical behavior of functionalized para-carboranes containing different azo-benzene derivatives on the alkyl-coated Au surface [43]. Thomas *et al.* examined geometries of carboxyl-functionalized para-carboranes on Au(111) by both experimental techniques and computational modeling [44]. Recent, scanning tunneling microscopy (STM) measurements of the SAMs indicate that the nearest-neighbor distances between the carboranethiol molecules are commensurate with the unreconstructed Au(111) [44,45]. Serino *et al.* investigated the adhesion properties of carborane isomers with various anchor groups on Ge surface [28]. The COOH anchor group was found to be more suitable than the thiol group for

*emete@balikesir.edu.tr

 ©2020 American Physical Society

carborane-based SAM structures on Ge surfaces. In addition, the work function of germanium with carborane carboxylate monolayers was shown to be modifiable in a 0.4 eV band without affecting the surface properties of germanium.

Utilization of functional groups with different electronic characteristics, particularly, for carborane-SAMs enables researchers to advance in selective bioapplications. For example, in a recent study, Neirynck *et al.* showed that RGD-functionalized carboranes on a full monolayer $\beta$-cyclodextrin-coated Au surface could detect C2C12-type cells [46]. In addition, some recent experimental studies have reported that the amphiphilic behavior of functionalized carborane derivatives is effective on some cancer cells [47,48].

A thorough understanding of the electronic and structural properties of carborane-based SAMs with functional groups is of great importance for development of novel applications. Computational studies are needed to bring new insights regarding the functionalized carborane-SAMs. In this study, we investigated the electronic and morphological structures of Au(111) in the presence of carborane isomers which are functionalized by COOH (as an acceptor group) and $NH_2$ (as a donor group) in the framework of dispersive-corrected density functional theory (vdW-DFT) simulations. We examined the role of the functional groups on the molecular dipole moments and, therefore, on the adsorption characteristics of carboranethiols on Au(111). Steric requirements due to position of the functional groups on the carboranethiol isomers play an active role on hexagonal molecular arrangement on the gold surface. In addition, the influence of the functional groups with counteracting electron affinities on the molecular dipole moments is determined in relation to tunability the work function of gold in the cases of isolated and monolayer carboranethiols.

## II. COMPUTATIONAL METHOD

Total energy density functional theory (DFT) calculations were performed within the framework of projector-augmented wave (PAW) method [49,50] as implemented in Vienna *ab initio* simulation package (VASP) [51,52]. Single-particle Kohn-Sham (KS) orbitals were expanded in the plane-wave basis up to a kinetic energy cutoff value of 400 eV. The exchange-correlation (XC) many-body effects and the van der Waals interactions were included using the meta-GGA SCAN+rVV10 functional [53].

To represent the Au surface, four-layer slab models with (111) surface termination was constructed by cleaving from bulk gold. Computational supercells include the gold slab, carboranethiol adsorbate(s) on the top layer and a 12 Å thick vacuum space along [111] direction. Convergence tests showed that the difference in the calculated binding energies between four and five layer slab models does not differ more than 2 meV. Each pure and functionalized carboranethiol isomer was considered as a single adsorbate on the Au(111)-(5×5) surface cell. The separation between the periodic images of a molecule is 13.72 Å which allows us to consider the carboranes to be isolated on the (5×5) structure. Possible adsorption sites were systematically examined for pure carborane derivatives previously [38]. In the cases of functionalized CTs, atop, bridge, and hollow sites were considered as the initial adsorption configurations. For the full monolayer, two possible conformations were taken into account. The first one involves a single CT on the (3×3). This dense packing arrangement allows hydrogen bonding since the functional group of one molecule gets closer to the boron vertex on the adjacent molecule. In the second one, two CTs are placed such that the functional groups form dimers which is commensurate with the (6×3) computational supercell. This conformation accepts a potential hydrogen bonding between the functional groups (COOH..COOH or $NH_2$..$NH_2$).

Brillouin zone integrations were carried out using Γ-centered 8×8×1, 4×8×1, and 5×5×1 $k$-point samplings for (3×3), (6×3), and (5×5) surface cells, respectively. A smearing parameter of 0.05 eV was set for Methfessel-Paxton (MP) scheme. Geometry optimizations of the model structures were obtained by minimization of the Hellmann-Feynman forces on each atom until a tolerance value of $10^{-2}$ eV/Å was reached in all spatial directions. The atoms at the bottom layer of the gold slab were frozen to their bulk positions.

The dissociative chemisorption energies, $E_c$, of pure and functionalized carboranethiol isomers on unreconstructed Au(111) with various periodicities can be calculated using,

$$E_c = \frac{E_{\mathrm{CT+Au(111)}} - E_{\mathrm{Au(111)}} - n(E_{\mathrm{CT}} - E_{\mathrm{H}})}{n},$$

where $E_{\mathrm{CT+Au(111)}}$ is the total energy of the supercell which contains the gold slab with $n$ number of CT adsorbates. $E_{\mathrm{Au(111)}}$ and $E_{\mathrm{CT}}$ are the total energy of the clean gold slab and the energy of a single CT molecule in a big box, respectively. The energy of an H atom, $E_{\mathrm{H}} = E_{\mathrm{H_2}}/2$, is calculated from molecular hydrogen.

The work function of Au(111) with functionalized CT adsorbates can be calculated as the difference between the vacuum level and the Fermi energy of the system. The vacuum level can be obtained from the planar-averaged electrostatic potential profiles along the surface normal ($z$-direction), which is given as

$$\overline{\mathrm{V}}(z) = \frac{1}{A} \iint_{\mathrm{cell}} V(x, y, z)\, dx\, dy,$$

where $V(x, y, z)$ is the real space electrostatic potential and $A$ is the area of the corresponding surface cell.

Charge transfer values from the gold surface to the adsorbate molecules were calculated based on the grid-based Bader analysis [54]. The change in the total charge of a molecule before and after adsorption was determined using

$$\Delta Q = Q_{\mathrm{CT(after\ adsorption)}} - Q_{\mathrm{CT(before\ adsorption)}}.$$

A positive value for $\Delta Q$ refers to electron transfer from the gold surface to the adsorbate molecule and vice versa. Since CT is considered to be dissociatively chemisorbed on the surface, the hydrogen atom which is attached at the thiol terminal is not present in the charge transfer calculations. $\Delta Q$ is given in units of $e$ which is the (fractional) number of electrons.

## III. RESULTS AND DISCUSSION

Optimized geometries of carboranethiol isomers were previously obtained using DFT calculations [38]. We follow the

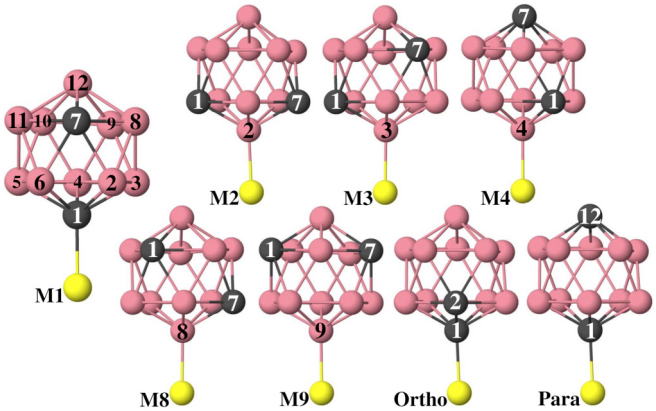


FIG. 1. Carboranethiol (CT) isomers are depicted in ball-and-stick form where pink, black and yellow balls represent boron, carbon and sulfur atoms. Hydrogen atoms are not shown for visual convenience. Labeling of meta isomers follows the attachment of thiol group on the carborane cage while keeping two carbon atoms at positions 1 and 7. The ortho (O) and para (P) variants differ from each other by the positioning of carbon atoms.

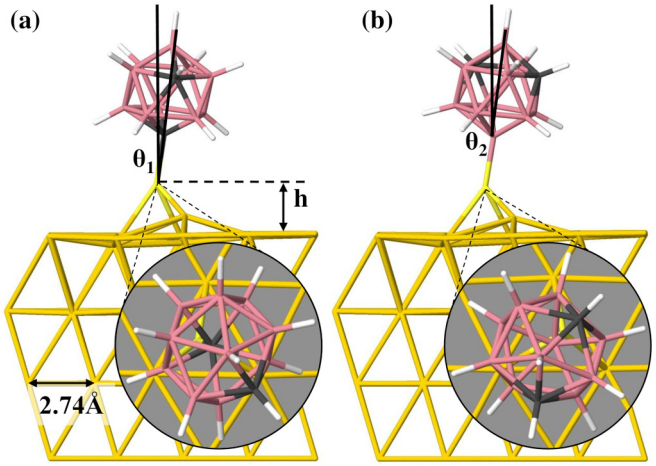


FIG. 2. Side and top (insets) views of (a) M1 and (b) M9 carboranethiol isomers on 5×5-Au(111) surface cell optimized using the SCAN+rVV10 DFT functional. The tilting angles of the S-cage bond and the major axis of the cage (with respect to the surface normal) are depicted on the models as $\theta_1$ and $\theta_2$, respectively. The height, $h$, indicates the separation between the S atom and the gold surface plane.

same labeling scheme of those positional isomers as presented in Fig. 1. In particular, metacarboranethiols are labeled with respect to the cage atom to which thiol group is attached. Placement of the functional groups depends on the positions of the two C atoms on the cage. There is only one possibility for M1, Ortho, and Para cases by construction and for M2 and M9 cases by symmetry. Two different attachment possibilities were considered for M3, M4, and M8. Among these two configurations, attachment of the functional groups to the carbon atom which is distant from the thiol part yields relatively lower energies on the gold surface. Therefore, carbon atom at position 7 on M3 and M4 and at position 1 on M8 were chosen for the placement of the functional groups. Recent experiments showed that ordered monolayers of COOH functionalized M1 and M9 carboranethiols are commensurate with the (5×5) and (3×3) unit cells of unreconstructed Au(111) [45].

### A. Isolated carboranethiols on Au(111)

A single isolated molecule was considered on Au(111)-(5×5) structure. The chemisorption of pure, COOH- and $NH_2$-functionalized CT isomers were systematically examined by considering possible initial adsorption sites which involve bridge, top and hollow positions on the (111) surface of gold as described for alkanethiols previously [39]. Geometry optimization computations based on the SCAN+rVV10 functional show that the thiol part of carborane derivatives plays a dominant role on the chemisorption site. The CT molecules are dragged by the S heads to a position on a triangle formed by three surface gold atoms, the hollow position. The S atom gets closer to bridge site forming two bonds with the bridging Au atoms. In this configuration, the S atom also forms a relatively shorter bond with the Au atom across the bridge site by lifting it up from the surface plane as shown in Fig. 2.

The (5×5) structure makes enough room for a separation of 13.72 Å between the periodic images of the S atoms, which corresponds to a low coverage adsorption case as depicted in Fig. 3. The S-Au bond lengths are consistent with covalent bond distances as given in Table I. Upon adsorption, the bond between the S atom and the carborane cage becomes tilted with respect to the surface normal, which is referred as $\theta_1$ as shown in Fig. 2. In most cases, the tilting of the cage itself, $\theta_2$, differs from $\theta_1$ as seen in Table I.

The bond length between the S atom and the carborane cage is affected by the attachment of the carboxyl and amine groups, only slightly. The bond distances are noticeably smaller for M1, Ortho (O), and Para (P) derivatives where S forms the bond with C atom of the cage. Therefore, the atomic species being either boron or carbon, to which the thiol group is attached on the carborane cage, can be identified as the main factor on the S-cage bonding.

However, both the functional groups and the molecular dipole moments (depending on the isomer type) become more important on the molecular adsorption and tilting angles on the (111) surface of gold. For instance, functionalized CT isomers get relatively more tilted on the gold surface at both low and high coverages. This situation is related to the molecular symmetry. The cage geometry of pure CT isomers are essentially the same. However, the terminal groups break the cylindrical symmetry. Therefore, functional groups not only bring additional charge but also lead to an asymmetrical charge distribution over the molecules. In addition, as the tilting increases, the carborane cage which has an outer diameter of ∼5.3 Å comes closer to the surface. As a results, a long range electronic interaction between the cage and the surface atoms contributes to the adsorption energy.

Four main factors can be considered, which influence the adsorption characteristics of the isolated CT molecules. These are the bonding between the thiol and surface gold atoms, the

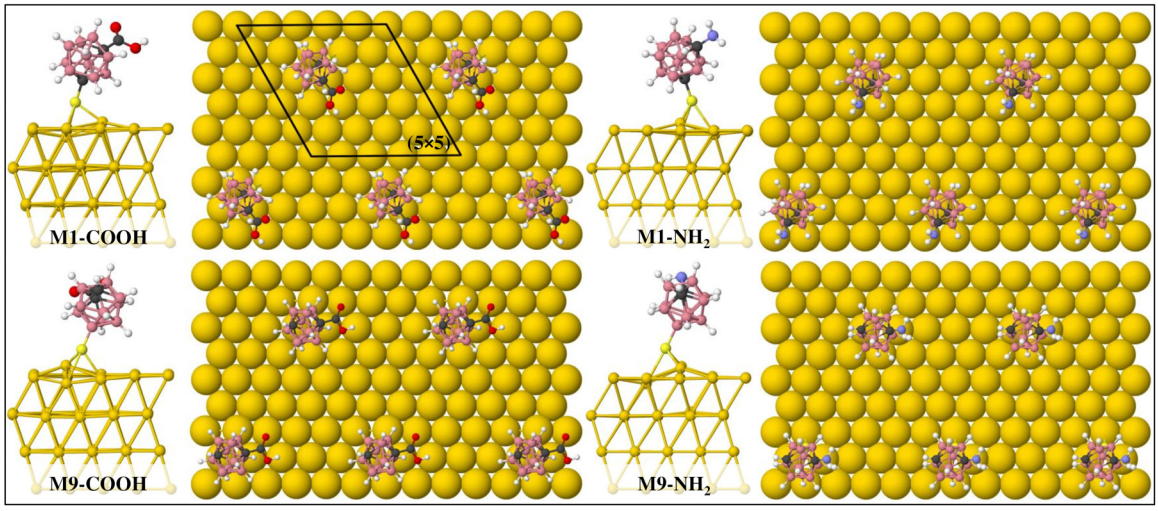


FIG. 3. The top and side views of COOH- and $NH_2$-functionalized M1 and M9 carboranes with (5×5) periodicity on Au(111). The structures were optimized using the SCAN+rVV10 functional. Yellow, gray, pink, red, and blue balls on the molecules represent S, C, B, O, and N atoms, respectively.

molecular dipole moment, the functional group, and the van der Waals interaction between the cage and the gold surface. The adsorption energies presented in Table I reveal that the strength and covalency of S-Au bonds are affected by the functional groups. For instance, the binding of M3-COOH variant is significantly stronger on the (5×5) structure. This case is also a good example which reflects the contribution of van der Waals interaction between the cage and the metal surface on its adsorption energy. The tilting of M3-COOH on the (5×5) structure is significantly larger among the other derivatives such that the closest distance from the cage to the gold surface becomes as small as 2.58 Å.

TABLE I. Structural parameters and adsorption energies of pure and functionalized carboranethiol (CT) isomers on Au(111)-(5×5) surface cell optimized by DFT calculations using the SCAN+rVV10 functional. Adsorption energies ($E_c$), bond lengths and heights ($d_{\text{S-Au}}$, $d_{\text{S-Cage}}$, h), and tilting angles ($\theta_1$, $\theta_2$) are given in units of eV, Å, and degrees, respectively.

| Molecule | $E_c$ | $d_{\text{S-Cage}}$ | $d_{\text{S-Au}}$ | $\theta_1$ | $\theta_2$ | h |
|---|---|---|---|---|---|---|
| M1 | −0.93 | 1.81 | 2.32, 2.65, 2.71 | 12.2 | 8.2 | 1.86 |
| M2 | −0.86 | 1.85 | 2.33, 2.62, 2.66 | 9.3 | 8.0 | 1.73 |
| M3 | −0.97 | 1.87 | 2.33, 2.62, 2.63 | 11.8 | 13.4 | 1.74 |
| M4 | −1.03 | 1.87 | 2.33, 2.48, 2.63 | 12.4 | 9.5 | 1.63 |
| M8 | −0.98 | 1.87 | 2.32, 2.52, 2.77 | 13.3 | 7.9 | 1.75 |
| M9 | −1.03 | 1.88 | 2.33, 2.51, 2.60 | 12.2 | 11.1 | 1.71 |
| O | −0.95 | 1.81 | 2.36, 2.48, 2.85 | 25.2 | 16.6 | 1.91 |
| P | −0.88 | 1.82 | 2.32, 2.75, 2.82 | 12.3 | 7.6 | 2.02 |
| M1-COOH | −1.20 | 1.81 | 2.36, 2.43, 2.92 | 29.6 | 21.0 | 1.91 |
| M2-COOH | −1.02 | 1.85 | 2.34, 2.47, 2.91 | 22.5 | 14.4 | 1.79 |
| M3-COOH | −1.60 | 1.86 | 2.42, 2.42, 3.05 | 42.3 | 38.0 | 1.96 |
| M4-COOH | −1.31 | 1.86 | 2.33, 2.42, 2.92 | 33.0 | 19.8 | 1.86 |
| M8-COOH | −1.06 | 1.86 | 2.38, 2.51, 2.82 | 26.8 | 15.2 | 1.92 |
| M9-COOH | −1.37 | 1.87 | 2.34, 2.42, 2.90 | 30.6 | 21.8 | 1.84 |
| O-COOH | −1.09 | 1.80 | 2.33, 2.55, 2.97 | 19.7 | 15.0 | 1.93 |
| P-COOH | −1.29 | 1.81 | 2.33, 2.43, 2.96 | 32.8 | 32.3 | 1.93 |
| M1-$NH_2$ | −1.02 | 1.81 | 2.34, 2.85, 2.91 | 28.4 | 22.1 | 2.12 |
| M2-$NH_2$ | −0.78 | 1.84 | 2.34, 2.50, 2.68 | 14.0 | 10.2 | 1.69 |
| M3-$NH_2$ | −1.21 | 1.87 | 2.35, 2.36, 2.86 | 27.7 | 25.2 | 2.07 |
| M4-$NH_2$ | −1.22 | 1.86 | 2.37, 2.41, 2.83 | 33.1 | 30.9 | 1.71 |
| M8-$NH_2$ | −1.14 | 1.86 | 2.33, 2.35, 2.81 | 20.3 | 9.7 | 1.92 |
| M9-$NH_2$ | −1.20 | 1.88 | 2.33, 2.35, 2.91 | 27.1 | 20.5 | 2.15 |
| O-$NH_2$ | −1.00 | 1.78 | 2.33, 2.90, 3.09 | 29.6 | 28.6 | 2.30 |
| P-$NH_2$ | −1.06 | 1.81 | 2.36, 2.72, 2.88 | 29.9 | 23.8 | 2.04 |

When the tilt angles, $\theta_1$ and $\theta_2$, of carborane derivatives in their computationally optimized structures are compared, CT molecules with amine or carboxyl functional groups appear to be tilted more relative to their pure counterparts. In addition, molecules which get strongly adsorbed on the metal surface have relatively higher tilting angles. Hence, presence of the functional groups can be related to the angle of tilting which shows a correlation with the binding energy, or with the stability, of CT derivatives on the metal surface. Among the pure isomers, the only exception seems to be the ortho (O) case. The nearest neighbor placement of C atoms at the positions 1 and 2 as shown in Fig. 1 causes an increased local electron density which leads to a molecular dipole moment, with a negative $z$ component (in Table II and Fig. 3), pointing toward the gold surface. This leads to a higher tilting angle relative to other pure isomers.

The position of functional groups change with the isomers depending on the positions of C atoms on the cage. In most cases, these groups are exposed on the surface. However, in some cases, these groups get closer to the metal surface upon chemisorption. For M2-COOH and O-COOH, the distance from the carboxyl to the surface is 4.05 Å and 4.09 Å, respectively. For M2-$NH_2$ and O-$NH_2$, these distances become 4.50 Å and 4.06 Å, respectively. Although these values are still large to consider a strong and direct interaction between the functional groups and the gold surface, positioning of the carboxyl and amine groups have an important role on the adsorption characteristics. Not only the tilting angles but also the functional groups increase steric demands of the CTs in the SAMs.

TABLE II. Dipole moment components (in units of Debye) of carboranethiol (CT) molecules, as adsorbed on the Au(111) with the (5×5) periodicity, calculated using the SCAN+rVV10 functional. The $z$-axis aligns with [111] direction and the $x$-axis is oriented along [101] direction. Work function values ($\Phi$ in eV) calculated for Au(111) with CT adsorbates (pure and functionalized) in the (5×5) surface structure. Charge transfer values ($\Delta Q$ in $e$) from the gold surface to individual molecules are given for their corresponding chemisorption geometries.

| Molecule | $\mu_x$ | $\mu_y$ | $\mu_z$ | $\Phi$ | $\Delta Q$ |
|---|---|---|---|---|---|
| M1 | −2.187 | −0.398 | 0.124 | 5.67 | 0.117 |
| M2 | −0.943 | −0.938 | −0.345 | 5.66 | 0.086 |
| M3 | 2.249 | −0.584 | 2.121 | 5.54 | 0.060 |
| M4 | −2.291 | 0.557 | 3.176 | 5.49 | 0.018 |
| M8 | −0.545 | 2.205 | 2.093 | 5.53 | 0.047 |
| M9 | 0.694 | −1.189 | 4.389 | 5.40 | 0.005 |
| O | −1.680 | 1.231 | −1.567 | 5.77 | 0.130 |
| P | −0.176 | −0.155 | 1.670 | 5.65 | 0.149 |
| M1-COOH | 0.549 | −2.207 | −0.721 | 5.74 | 0.091 |
| M2-COOH | 0.812 | −2.617 | −0.196 | 5.72 | 0.107 |
| M3-COOH | −1.252 | −2.413 | 1.195 | 5.70 | 0.042 |
| M4-COOH | 0.207 | 1.870 | 3.517 | 5.59 | 0.021 |
| M8-COOH | −1.823 | −1.201 | 0.825 | 5.69 | 0.086 |
| M9-COOH | 0.823 | −1.605 | 4.459 | 5.49 | −0.007 |
| O-COOH | −0.917 | −1.939 | −1.959 | 5.80 | 0.200 |
| P-COOH | 1.325 | 0.522 | 1.227 | 5.71 | 0.083 |
| M1-$NH_2$ | −1.686 | −2.133 | 1.038 | 5.80 | 0.119 |
| M2-$NH_2$ | 1.033 | −1.611 | 0.202 | 5.79 | 0.049 |
| M3-$NH_2$ | 2.969 | −1.649 | 2.034 | 5.69 | −0.010 |
| M4-$NH_2$ | −4.780 | −0.113 | 2.108 | 5.63 | 0.012 |
| M8-$NH_2$ | 1.266 | 1.189 | 3.580 | 5.57 | 0.014 |
| M9-$NH_2$ | 0.464 | −0.201 | 4.121 | 5.54 | −0.029 |
| O-$NH_2$ | −2.518 | −0.574 | −2.735 | 5.92 | 0.115 |
| P-$NH_2$ | −0.425 | −0.746 | 3.200 | 5.75 | 0.109 |

Molecular dipole moments were calculated to explore their effect on the binding energies. For this purpose, CT molecules were considered in big computational boxes for which the $z$ and $x$ axes are chosen to coincide with the [111] and [101] directions of the gold slab. Then, the calculations of the molecular dipole moments were performed using the frozen atomic coordinates in their corresponding dissociative adsorbed-state geometries. To provide comparability of the dipole moments between different chemisorption geometries, H atoms were not attached at the thiol terminals. The results for (5×5) cases are presented in Table II. Previous studies emphasized the role of molecular dipoles on the formation and stability of CTs on Au(111) by considering pure M1 and M9 positional isomers. Although they have similar geometrical shapes, M1 and M9 possess molecular dipole orientations almost parallel and perpendicular to the gold surface with moments of 1.06 D and 4.08 D in the gas phase, respectively [19]. Our results show that M1 and M9 isomers essentially keep their gas phase dipole orientations even though they get slightly tilted after chemisorption on the gold surface at low density (5×5) hexagonal packing. The binding energies show a correlation with both the dipole moments and their orientations. A larger dipole

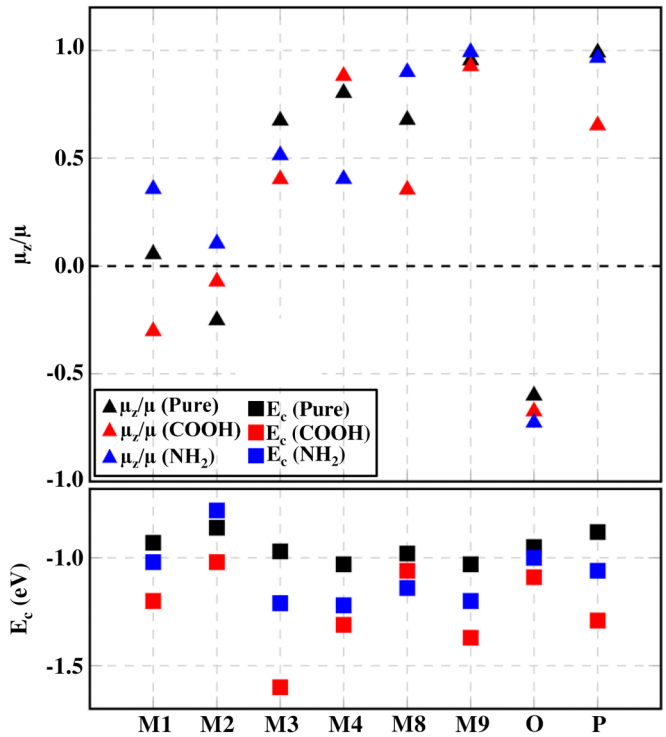


FIG. 4. DFT-calculated $z$ components (corresponding to [111] direction gold surface) of molecular dipoles normalized to their net moments ($\mu_z/\mu$) and the chemisorption energies ($E_c$) of pure and functionalized carboranethiols on the Au(111)-(5×5) using the SCAN+rVV10 functional.

with a sizable component along surface normal leads to a relatively stronger chemisorption. The dipole components perpendicular to the surface normalized to the net dipole moments ($\mu_z/\mu$) and chemisorption energies ($E_c$) are depicted in Fig. 4 for all adsorption cases of pure isomers on the (5×5) supercell. Indeed, the weakest adsorption occurs for M2 isomer among the pure and functionalized cases, which has the smallest dipole component along [111]. As a trend for the cases with moderate tilting angles, a molecular dipole parallel to the metal surface gives a slightly weaker binding relative to that perpendicular to the surface in the $+z$ direction ([111] direction relative to underlying gold).

The CT molecules bind significantly stronger to the gold surface with the attachment of both of the functional groups. In fact, the nominal charge states of COOH and $NH_2$ groups in a chemical environment are different, the former being an electron acceptor and the latter being an electron donor group. The amine moiety enhances adsorption of carboranes isomers on gold relative to their corresponding pure cases with the only exception of M2. In particular, carboxylic acid group makes carboranes to bind to the gold surface even slightly stronger relative to the amine group. The change in the binding energy is in the range between 0.14 eV (for O) and 0.63 eV (for M3). The role of charge transfers from CT molecules to the gold substrate were considered and the calculated values are given in Table II. It appears that CT molecules, functionalized or not, get slightly reduced upon

adsorption in most of the cases. The amount of charge transfer from the gold surface to the CTs seems to be affected mainly by the positional isomerization. The results indicate that the type of the terminal functional group is less effective in S-Au bonding characteristics.

For the isolated case, the adsorption characteristics of pure CT isomers determined by the SCAN+rVV10 functional can be compared with previous optB86b-vdW results [38]. The SCAN+rVV10 functional predicted CT isomers to be staying relatively higher above the gold surface plane. In fact, these two different DFT approaches do not end up with identical adsorption geometries as there are also noticeable differences between the calculated bonds. In relation to final geometries, the SCAN+rVV10 functional gives relatively weaker binding of CT isomers on gold due to its differences with the optB86b-vdW functional in the formalisms of the XC effects and the dispersive forces.

DFT calculations using SCAN+rVV10 functional predicts a work function of the bare Au(111) as 5.41 eV [55] which is reasonably acceptable when compared with the experimentally estimated value of $5.33 \pm 0.06$ eV [56]. Experimental studies reported a change in the work function with M9 monolayers on gold [19,27]. The influence was considerably smaller in the case of M1 [19]. The change in the work function is attributed to the molecular dipole moments and their orientations on the gold surface. Since M9 has a considerably larger dipole moment relative to that of M1, and since its dipole points almost perpendicular to the surface, M9 adsorption has a larger influence on the work function. In fact, adsorbates with a dipole with a positive pole pointing away from the surface cause a decrease in the work function. The effect, even, reverses if the negative pole points away from the surface [16–18]. To examine the role of the functional groups on the work function, we first considered all the isomers on the (5×5) structure as given in Table II. In consistency with the observations of Kim *et al.* [27], the lowest work function was obtained for M9 among pure CT isomers. Our calculations indicate an increase in the work function by chemisorption of CT molecules with dipoles aligning parallel to the gold surface as in the cases of M1 and M2. The most dramatic increase happens for the adsorption of ortho-CT which has a dipole almost opposite to M9. A similar influence of dipole moments on the work function is also seen for the functionalized CTs. The both functional groups lead to an increase in the work function of gold relative to the pure cases. The change is noticeably larger with the amine functional group relative to carboxyl functional group. Adsorption of M4-COOH and M9-COOH gives considerably lower work function among the carboxyl functionalized CTs. Similarly, M8-$NH_2$ and M9-$NH_2$ isomers have the two lowest the work functions among the amine functionalized CTs as they possess the largest dipole moment component along surface normal. The results for the isolated cases indicate that pure and functionalized derivatives of M1, M2, and O CTs cause noticeably higher work function among the other isomers, as expected, depending on their dipole moments and orientations. The functional groups have an observable effect which allows a wider range for the tunability of the work function of gold.

### B. Carboranethiol monolayers on Au(111)

Recent STM measurements on SAMs of M1-COOH and M9-COOH on Au(111) gave nearest-neighbor distances of $8.4 \pm 0.4$ Å for both isomers [45]. Densely packed monolayers of carboranethiols are commensurate with the (3×3) unit cell of unreconstructed Au(111) where computational nearest-neighbor separation is 8.23 Å. Due to shorter spacing of molecules and steric requirements in the presence of functional groups, tilting angles can be expected to be smaller than that of the isolated cases. The M1 and M9 isomers were taken into account for SAM structures by many experiments in the first place due to their dipoles which are oriented parallel and perpendicular to the gold surface, respectively. Therefore, we focus on these isomers which reflect contrasting dipole orientations as favorable candidates to investigate the effect of carboxyl and amine functional groups on the characteristics of SAMs. Moreover, the adsorption geometries and binding energies can be compared in relation to possible dipole-dipole interactions in the monolayers.

On the (3×3) structure two possible initial configurations can be considered. In the first one molecules are tilted backwards to expose the functional groups on the monolayer to the environment. The second one corresponds to the molecule tilting forward as shown in Fig. 5. In this conformation each CT molecule with the functional group lean toward the neighboring molecule allowing a possibility of hydrogen interaction in the lateral direction. For M1-COOH, the latter configuration is energetically 0.1 eV more favorable than the former one. Hence, computationally both structures are expected to be stable. Experiments reported that the two conformations are indistinguishable under STM measurements [45]. An initial configuration with the first conformation relaxes to the second one in the cases of M9-COOH, M1-$NH_2$ and M9-$NH_2$ on the (3×3) unit cell.

Instead of functional groups facing the same direction in the monolayer, an alternating arrangement is possible where every two neighboring molecules face each other allowing the functional groups to form dimers. This type of intermolecular interaction corresponds to the (6×3) unit cell with respect to the underlying gold substrate, as shown in Fig. 6. The nearest-neighbor distance becomes 9.21 Å between the molecules whose functional groups show dimer formation with increased steric demands while it is 7.95 Å between molecules with non-dimering functional groups along the other lateral direction. Therefore, resulting molecular ordering breaks the uniformity of the adlayer morphology.

On the (3×3) structure, the shortest distance between the carboxyl proton to the boron vertex on the adjacent molecule in the lateral direction is 2.59 Å and 2.75 Å for M1 and M9, respectively. Hence, COOH..BH hydrogen bonding is more favorable and has a larger effect on the adsorption characteristics. In the case of the amine group, these distances are 3.49 Å and 3.35 Å, for M1 and M9 isomers, respectively. On the (6×3) structure, the protons mutually interact with the adjacent oxygens of the dimering carboxylic acids. The O-H distances are 1.56 Å for M1-COOH and 1.55 Å for M9-COOH. The separations between $NH_2$ dimers are 3.06 Å for M1-$NH_2$ and 3.42 Å for M9-$NH_2$. Therefore, intermolecular interactions between the dimering molecules are more

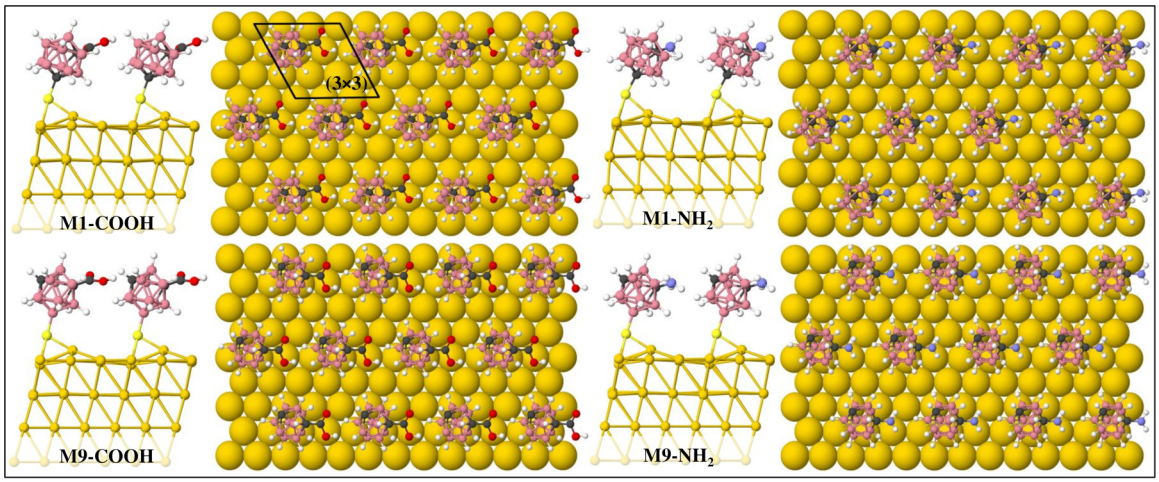


FIG. 5. The top and side views of COOH- and $NH_2$-functionalized M1 and M9 carboranes with (3×3) periodicity on Au(111). The structures were optimized using the SCAN+rVV10 functional. Yellow, gray, pink, red, and blue balls on the molecules represent S, C, B, O, and N atoms, respectively.

pronounced in the case of COOH-functionalized (6×3) structures. In fact, COOH-dimer conformation gives the strongest binding among the other probable adsorption structures as seen in Table III.

Pure and functionalized carboranethiols chemisorp at the threefold hollow site both on (3×3) and (6×3) unit cells in agreement with experiments [19,45]. Isolated molecules, however, tend to be adsorbed closer to the bridge site. As a common feature for all coverage models, the S atom lifts one of the threefold coordinated gold atoms from surface plane leading to a significantly shorter S-Au bond relative to the other two. This causes a local distortion around the chemisorption site which is particularly more pronounced in the densely packed arrangements relative to that of the isolated molecules. The S-Au and S-Cage bonds reflect typical distances similar to the isolated cases as seen in Table III. As a result, the thiol plays an important role as an anchor between the gold surface and the carborane monolayer. Furthermore, neither attachment of the functional groups nor increased molecular density on the gold surface appear to noticeably influence the skeletal stability of the molecules.

The tilting angles are expected to be reduced due to both increased molecular density in the monolayers and steric preferences of functionalized CTs. Indeed, a decrease of the tilting angles is seen for molecules leaning toward their nearest-neighbors forming the (3×3) structure. Particularly, the comparison between the (5×5) and (3×3) cases shows that the most significant reduction in the tilting angles happens for the pure and functionalized M9 isomers due mainly to stronger intermolecular forces. The interactions between the M1 isomers are weaker, because they have considerably smaller dipole moments with orientations almost parallel to the surface as presented in Table IV. Contrary to (3×3) cases, the molecules in dimer formation on (6×3) cell get even more tilted relative to isolated molecules on the (5×5) structure. In the case of pure isomers, molecules are not tilted

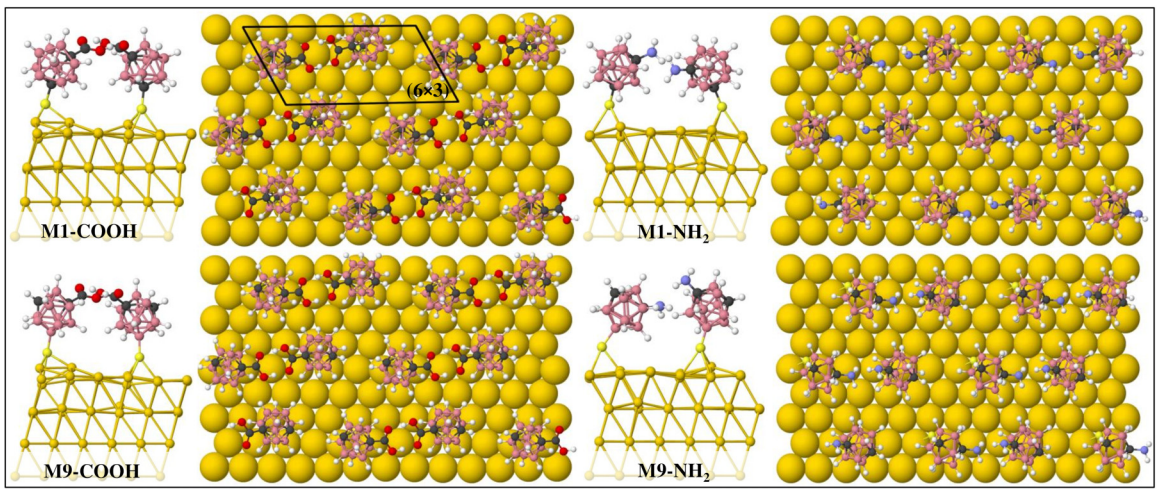


FIG. 6. The top and side views of COOH- and $NH_2$-functionalized M1 and M9 carboranes with (6×3) periodicity on Au(111). The structures were optimized using the SCAN+rVV10 functional. Yellow, gray, pink, red, and blue balls on the molecules represent S, C, B, O, and N atoms, respectively.

TABLE III. Structural parameters and energetics of pure and functionalized M1 and M9 carboranes on the (3×3) and (6×3) surface cells with respect to Au(111) calculated using the SCAN+rVV10 XC functional. Adsorption energies ($E_c$), bond lengths and heights ($d_{S\text{-}Au}$, $d_{S\text{-}Cage}$, h), and tilting angles ($\theta_1$, $\theta_2$) are given in units of eV, Å, and degrees, respectively.

| Molecule | $E_c$ | $d_{S\text{-}Cage}$ | $d_{S\text{-}Au}$ | $\theta_1$ | $\theta_2$ | h |
|---|---|---|---|---|---|---|
| | | | CT/Au(111)-(3×3) | | | |
| M1 | −1.31 | 1.80 | 2.31, 2.66, 2.75 | 10.7 | 5.2 | 1.97 |
| M9 | −1.23 | 1.85 | 2.31, 2.62, 2.63 | 7.1 | 2.1 | 1.91 |
| M1-COOH | −1.57 | 1.80 | 2.33, 2.73, 2.85 | 21.6 | 16.7 | 2.17 |
| M9-COOH | −1.60 | 1.86 | 2.33, 2.59, 2.76 | 15.5 | 10.5 | 2.09 |
| M1-$NH_2$ | −1.51 | 1.80 | 2.34, 2.78, 2.92 | 30.1 | 24.9 | 2.25 |
| M9-$NH_2$ | −1.45 | 1.86 | 2.34, 2.53, 2.87 | 23.1 | 15.4 | 2.14 |
| | | | CT/Au(111)-(6×3) | | | |
| M1 | −1.38 | 1.81 | 2.34, 2.95, 2.97 | 28.3 | 22.8 | 2.36 |
| | | 1.80 | 2.32, 2.97, 3.17 | 29.6 | 24.1 | 2.42 |
| M9 | −1.38 | 1.81 | 2.37, 2.75, 2.82 | 30.3 | 27.3 | 2.26 |
| | | 1.81 | 2.40, 2.65, 2.84 | 30.5 | 25.4 | 2.15 |
| M1-COOH | −1.91 | 1.81 | 2.33, 2.36, 2.98 | 30.1 | 23.5 | 2.36 |
| | | 1.81 | 2.33, 2.53, 2.80 | 17.3 | 8.7 | 1.97 |
| M9-COOH | −1.90 | 1.86 | 2.33, 2.36, 2.86 | 20.5 | 12.4 | 2.24 |
| | | 1.86 | 2.39, 2.52, 2.80 | 21.2 | 13.9 | 1.87 |
| M1-$NH_2$ | −1.59 | 1.80 | 2.36, 2.91, 2.94 | 32.2 | 27.2 | 1.87 |
| | | 1.80 | 2.35, 2.93, 3.00 | 33.6 | 28.4 | 2.02 |
| M9-$NH_2$ | −1.55 | 1.86 | 2.37, 2.88, 2.98 | 36.3 | 28.8 | 2.29 |
| | | 1.86 | 2.35, 2.74, 2.86 | 28.4 | 20.5 | 2.21 |

toward each other. They become oppositely tilted. However, dimering carboxyl and amine groups cause the CTs to lean toward each other due to hydrogen bonding between them. The (3×3) and (6×3) conformations allow different hydrogen bonding possibilities between the functionalized CTs. The dimer conformation in which more positively charged part of a functional group facing more negatively charged part of the adjacent group at a distance of 1.54 Å builds an attractive force between the nearest-neighbor molecules, allowing them to lean more toward each other on the surface.

As going from isolated to full monolayer coverages, calculated dissociative chemisorption energies show stronger binding between the CT molecules and the gold surface due to intermolecular interactions in monolayers. Furthermore, the functional groups have significant influence on the binding energies. In particular, carboxyl acid group appears to be more effective to get more stable monolayers relative to the amine group. This is particularly noticeable in the COOH attached carborane coating on the (6×3) cell of Au(111). The chemisorption energies of M1 and M9 isomers with the same functional group become almost indistinguishable, which allows a possibility of mixed monolayer realization.

The charge transfer from the gold surface to CTs is mainly characterized by positional isomerization which modifies molecular dipole moments. The amount of charge transfer for M9 derivatives is slightly smaller than that of M1. In addition, as the molecular density increases from isolated to full monolayer coverage, a noticeable increase is seen in the amount of charge transfer per molecule. Such an increasing charge transfer corresponds to a stronger binding in favor of dense packing. Moreover, the functional groups appear to have a secondary effect on the charge transfer values. Molecular dipoles are useful in modifying the work function of gold. Kim *et al.* reported that the work function of gold decreases with M9 coverage and increases with M1 adsorption. A similar trend in the calculated work function values

TABLE IV. Dipole moment components ($\mu_x$, $\mu_y$, $\mu_z$ in D) of pure and functionalized carboranethiols calculated using the same molecular orientations on Au(111) with (3×3) and (6×3) cell structures. The $z$-axis corresponds to the [111] direction and the $x$ axis is oriented along [101] direction. Work function values ($\Phi$ in eV) calculated for CT/Au(111) systems at full monolayer coverage. Charge transfers values ($\Delta Q$ in $e$) from the gold surface to individual molecules are given for their corresponding chemisorption geometries.

| Molecule | $\mu_x$ | $\mu_y$ | $\mu_z$ | $\Phi$ | $\Delta Q$ |
|---|---|---|---|---|---|
| | | | CT/Au(111)-(3×3) | | |
| M1 | −0.332 | −2.125 | 0.526 | 5.50 | 0.175 |
| M9 | −0.641 | −1.333 | 4.270 | 4.96 | 0.096 |
| M1-COOH | 1.945 | −0.949 | 0.204 | 5.57 | 0.160 |
| M9-COOH | 0.889 | −0.417 | 3.542 | 5.10 | 0.103 |
| M1-$NH_2$ | 2.822 | −0.023 | −0.256 | 5.66 | 0.146 |
| M9-$NH_2$ | 2.551 | 1.424 | 3.220 | 5.17 | 0.083 |
| | | | CT/Au(111)-(6×3) | | |
| M1 | 2.086 | 0.357 | 0.610 | 5.52 | 0.148 |
| | −4.231 | 0.448 | 0.627 | | 0.169 |
| M9 | 0.010 | −0.615 | 4.421 | 4.99 | 0.109 |
| | −0.014 | 3.188 | 3.257 | | 0.097 |
| M1-COOH | 2.281 | −1.220 | −0.424 | 5.58 | 0.111 |
| | −2.229 | 1.235 | 0.248 | | 0.149 |
| M9-COOH | 0.487 | −1.440 | 3.358 | 5.13 | 0.052 |
| | 0.089 | −1.440 | 3.912 | | 0.113 |
| M1-$NH_2$ | 2.448 | −1.468 | 0.638 | 5.67 | 0.150 |
| | −2.617 | 1.049 | −0.329 | | 0.165 |
| M9-$NH_2$ | 2.582 | −0.596 | 2.939 | 5.15 | 0.116 |
| | 0.533 | −1.388 | 4.507 | | 0.121 |

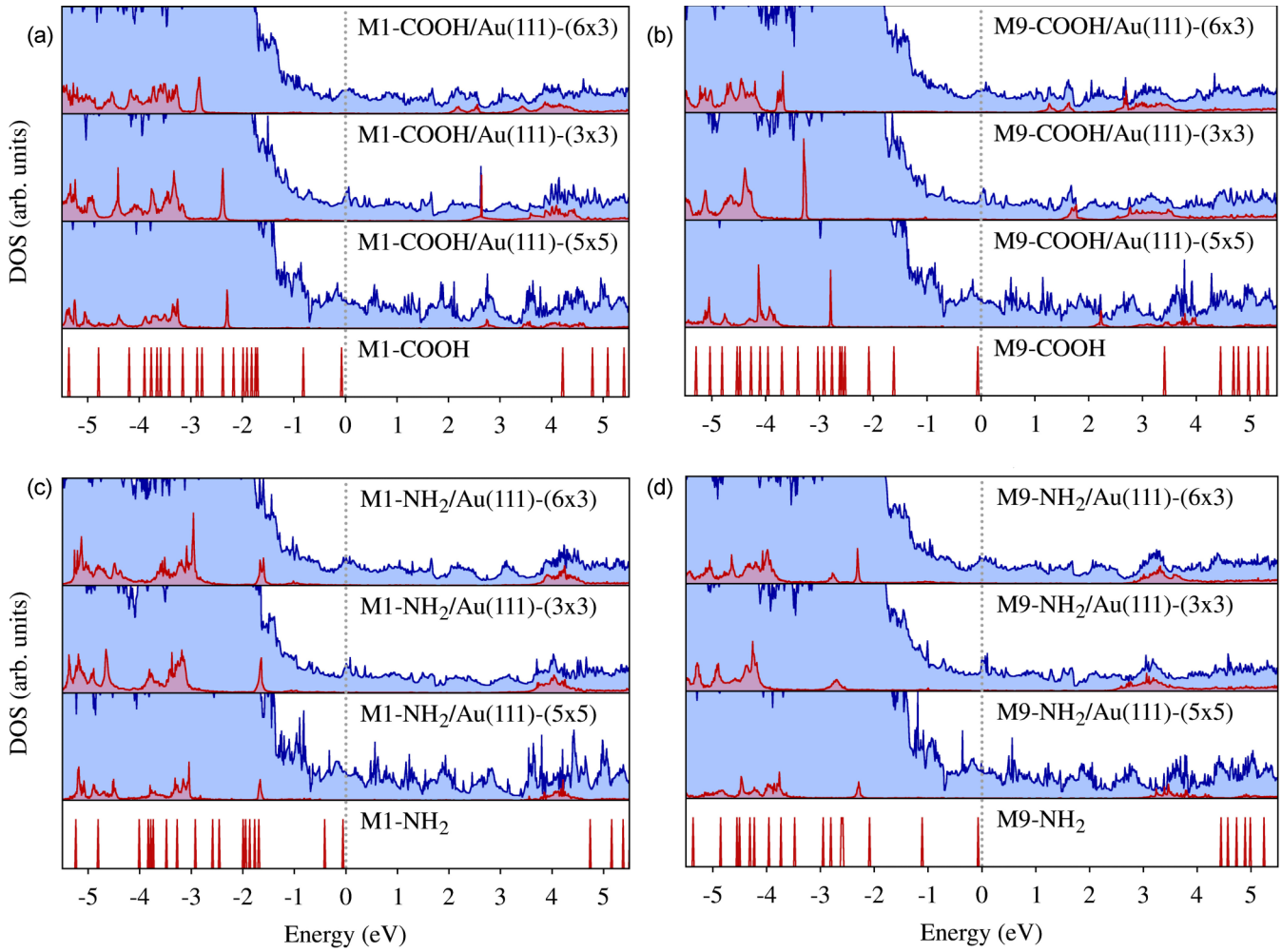


FIG. 7. Molecular partial (red) and total (blue) densities of states for (a) M1COOH, (b) M9COOH, (c) M1NH$_2$, and (d) M9NH$_2$ on Au(111) with (5×5), (3×3), and (6×3) structures calculated using the SCAN+rVV10 functional. The bottom panels show the energy levels of the corresponding isomers in the gas phase. Vertical dashed lines indicate the Fermi energy for each system.

is seen in Tables II and IV. In consistency with experimental measurements, a monolayer of M9 decreases the work function by 0.45 eV relative to that of the bare Au(111) while a monolayer of M1 increases it by 0.09 eV in the case of (3×3) cell. Similar results were obtained for carboranethiol SAMs with the (6×3) cell. Experiments demonstrated tunability of the work function by depositing mixed SAMs with varying concentrations of M1 and M9 isomers [27]. In addition, a comparison between the isolated and monolayer cases indicate that increasing molecular density reduces the the work function of gold. The reduction is ∼0.2 eV and ∼0.4 eV for M1 and M9 isomers. Both carboxylic acid and amine functional groups are effective in modifying the work function relative to pure M1 and M9 monolayers on gold. These groups not only offer a modifiability of the work function over a wider range but also play an important role in the formation of well-ordered and functional SAMs for various applications.

### C. Electronic structures of carboranethiols on Au(111)

The electronic densities of states (DOS) with partial projections were calculated for isolated and monolayer CTs on unreconstructed Au(111). The M1 and M9 isomers with amine and carboxyl functional groups considered as presented in Fig. 7. The DOS structures for different unit cells were aligned with respect to deep core states. In the gas phase, M1-NH$_2$ and M9-NH$_2$ have HOMO-LUMO separations of 4.7 and 4.4 eV, respectively.While the separation between the frontier orbitals is 4.2 eV for M1-COOH, it is significantly smaller for M9-COOH as being 3.3 eV.

Chemisorption of amine and carboxyl functionalized CTs on Au(111) has a drastic influence on the frontier molecular orbitals. The partial DOS (PDOS) structures show that the HOMO levels strongly resonate over a wide range of the occupied gold states as a result of the bond formation between the thiol terminal and the surface gold atoms. Upon adsorption, the HOMO-1 and LUMO states broaden and shift down more than 1 eV to lower energies. The shift increases going from the isolated to the monolayer phases, especially, in favor of the dimer conformation on the (6×3) cell in consistency with the calculated chemisorption energies. Moreover, this effect for both occupied and unoccupied DOS features is particularly more pronounced in the carboxylated CT cases.

The main PDOS features of amine functionalized M1 and M9 molecules are essentially kept as going from isolated

(5×5) to monolayer (3×3) and (6×3) coverages. In particular, for M1-$NH_2$, the HOMO-1 at around −2 eV, a satellite of occupied molecular states in the interval between −3 eV and −5.5 eV, and a group of antibonding molecular states centered around 4 eV, basically keep their positions and forms throughout different coverages and conformations. Slight changes between the PDOS of $NH_2$ functionalized isomers on gold can be attributed to relatively weaker intermolecular interactions. In the case of carboxyl functionalized CTs on the gold surface, the shifting and broadening of both occupied and unoccupied energy states associated with the CTs increase depending on the molecular density. Dense packing of COOH functionalized CTs gives rise to hydrogen bonding and favorable dipole-dipole interactions between neighboring molecules within the monolayers.

## IV. CONCLUSIONS

The functional groups bring anisotropy to CTs and increase their steric requirements depending on positional isomerization. The DFT calculations including vdW effects reveal that thiol heads form an inequivalent threefold coordination with the gold atoms. Isolated molecules relax closer to bridge site while densely packed molecules prefer the hollow site. One of the surface gold atoms raised up from the surface plane by the thiol terminal causing a tilted adsorption. The tilt relative to the surface normal and the absolute value of chemisorption energies increase with the functional groups. The change in the chemisorption energies favors high molecular density. Therefore, the DFT calculations indicate that functionalization of CT isomers lead to more stable monolayers on the gold surface. Carboxylic acid group is slightly more effective than amine group, in increasing the absolute value of dissociative chemisorption energies.

In addition to the cage geometry of carboranethiols, adsorption geometries and energies are mainly characterized by the bonding between the thiol and surface gold atoms, the molecular dipole moments and the functional groups. The results clearly show the effect of intermolecular interactions which are effective in the densely packed arrangements. Presence of functional groups make two different conformations probable for monolayer structures. The functional groups align in the same lateral direction or form dimers facing each other, which are commensurate with the (3×3) and (6×3) cells with respect to underlying Au(111). These dense packing conformations give rise to hydrogen bonding and favorable dipole-dipole interactions in monolayers.

The functional groups in conjunction with positional isomerization influence the molecular dipole moments. A dipole along surface normal decreases the work function while a dipole parallel to the surface plane increases it. The functional groups, which are exposed to the environment from the SAM surfaces, have different electrochemical responses allowing various designs for applications. Therefore, the carboxyl and amine groups are useful in functionalization of SAM structures and still offer tunability of the work function with desirable properties.

Although amine and carboxyl groups have different electronic charge states one being an electron donor and the other being an electron acceptor, they both make CT molecules to bind to the gold surface stronger. More studies are needed to explore the effect of other possible functional groups on the characteristics of SAMs.

## ACKNOWLEDGMENTS

This study was supported by Tubitak, The Scientific and Technological Research Council of Turkey (Grant No. 116F174) and Balıkesir University (Project No. BAP 2018/039). The calculations that conducted in this article have been performed on the High Performance and Grid Computing Center (TRUBA parallel computer center).

[1] A. Kumar, H. A. Biebuyck, and G. M. Whitesides, Langmuir **10**, 1498 (1994).
[2] A. R. Bishop and R. G. Nuzzo, Curr. Opin. Colloid Interface Sci. **1**, 127 (1996).
[3] J. H. Schön, H. Meng, and Z. Bao, Nature **413**, 713 (2001).
[4] J. H. Fendler, Chem. Mater. **13**, 3196 (2001).
[5] N. K. Chaki and K. Vijayamohanan, Biosens. Bioelectron. **17**, 1 (2002).
[6] J. J. Gooding, F. Mearns, W. Yang, and J. Liu, Electroanalysis **15**, 81 (2003).
[7] J. C. Love, L. A. Estroff, J. K. Kriebel, R. G. Nuzzo, and G. M. Whitesides, Chem. Rev. **105**, 1103 (2005).
[8] M. Frasconi, F. Mazzei, and T. Ferri, Anal. Bioanal. Chem. **398**, 1545 (2010).
[9] C. Vericat, M. Vela, G. Benitez, P. Carro, and R. Salvarezza, Chem. Soc. Rev. **39**, 1805 (2010).
[10] D. Mandler and S. Kraus-Ophir, J. Solid State Electrochem. **15**, 1535 (2011).
[11] B. de Boer, A. Hadipour, M. M. Mandoc, T. van Woudenbergh, and P. W. Blom, Adv. Mater. **17**, 621 (2005).
[12] T. Baše, Z. Bastl, Z. Plzák, T. Grygar, J. Plešek, M. J. Carr, V. Malina, J. Šubrt, J. Boháček, E. Večerníková *et al.*, Langmuir **21**, 7776 (2005).
[13] S. Balaz, A. N. Caruso, N. P. Platt, D. I. Dimov, N. M. Boag, J. I. Brand, Y. B. Losovyj, and P. A. Dowben, J. Phys. Chem. B **111**, 7009 (2007).
[14] N. Gozlan, U. Tisch, and H. Haick, J. Phys. Chem. C **112**, 12988 (2008).
[15] T. Baše, Z. Bastl, M. Šlouf, M. Klementová, J. Šubrt, A. Vetushka, M. Ledinský, A. Fejfar, J. Macháček, M. J. Carr, and M. G. S. Londesborough, J. Phys. Chem. C **112**, 14446 (2008).
[16] X. Crispin, V. Geskin, A. Crispin, J. Cornil, R. Lazzaroni, W. R. Salaneck, and J.-L. Brédas, J. Am. Chem. Soc. **124**, 8131 (2002).
[17] R. W. Zehner, B. F. Parsons, R. P. Hsung, and L. R. Sita, Langmuir **15**, 1121 (1999).

[18] H. Ishii, K. Sugiyama, E. Ito, and K. Seki, Adv. Mater. **11**, 605 (1999).
[19] J. N. Hohman, P. Zhang, E. I. Morin, P. Han, M. Kim, A. R. Kurland, P. D. McClanahan, V. P. Balema, and P. S. Weiss, ACS Nano **3**, 527 (2009).
[20] S.-H. Lee, W.-C. Lin, C.-J. Chang, C.-C. Huang, C.-P. Liu, C.-H. Kuo, H.-Y. Chang, Y.-W. You, W.-L. Kao, G.-J. Yen *et al.*, Phys. Chem. Chem. Phys. **13**, 4335 (2011).
[21] J. F. Lübben, T. Baše, P. Rupper, T. Künniger, J. Macháček, and S. Guimond, J. Colloid Interface Sci. **354**, 168 (2011).
[22] F. Scholz, H.-G. Nothofer, J. M. Wessels, G. Nelles, F. von Wrochem, S. Roy, X. Chen, and J. Michl, J. Phys. Chem. C **115**, 22998 (2011).
[23] T. Baše, Z. Bastl, V. Havránek, K. Lang, J. Bould, M. G. S. Londesborough, J. Macháček, and J. Plešek, Surf. Coat. Technol. **204**, 2639 (2010).
[24] T. Baše, Z. Bastl, V. Havránek, J. Macháček, J. Langecker, and V. Malina, Langmuir **28**, 12518 (2012).
[25] E. Albayrak, S. Duman, G. Bracco, and M. Danışman, Appl. Surf. Sci. **268**, 98 (2013).
[26] E. Albayrak, S. Karabuga, G. Bracco, and M. F. Danışman, Appl. Surf. Sci. **311**, 643 (2014).
[27] J. Kim, Y. S. Rim, Y. Liu, A. C. Serino, J. C. Thomas, H. Chen, Y. Yang, and P. S. Weiss, Nano Lett. **14**, 2946 (2014).
[28] A. C. Serino, M. E. Anderson, L. M. A. Saleh, R. M. Dziedzic, H. Mills, L. K. Heidenreich, A. M. Spokoyny, and P. S. Weiss, ACS Appl. Mater. Interfaces **9**, 34592 (2017).
[29] A. Yavuz, N. Sohrabnia, A. Yilmaz, and M. F. Danışman, Appl. Surf. Sci. **413**, 233 (2017).
[30] B. Foerster, V. A. Spata, E. A. Carter, C. Sönnichsen, and S. Link, Sci. Adv. **5**, eaav0704 (2019).
[31] H. Grönbeck, A. Curioni, and W. Andreoni, J. Am. Chem. Soc. **122**, 3839 (2000).
[32] P. C. Rusu and G. Brocks, Phys. Rev. B **74**, 073414 (2006).
[33] P. C. Rusu, G. Giovannetti, and G. Brocks, J. Phys. Chem. C **111**, 14448 (2007).
[34] L. Romaner, G. Heimel, and E. Zojer, Phys. Rev. B **77**, 045113 (2008).
[35] M. L. Sushko and A. L. Shluger, Adv. Mater. **21**, 1111 (2009).
[36] D. Otálvaro, T. Veening, and G. Brocks, J. Phys. Chem. C **116**, 7826 (2012).
[37] S. Osella, D. Cornil, and J. Cornil, Phys. Chem. Chem. Phys. **16**, 2866 (2014).
[38] E. Mete, A. Yılmaz, and M. F. Danışman, Phys. Chem. Chem. Phys. **18**, 12920 (2016).
[39] E. Mete, M. Yortanlı, and M. F. Danışman, Phys. Chem. Chem. Phys. **19**, 13756 (2017).
[40] D. Cornil and J. Cornil, J. Electron Spectrosc. Relat. Phenom. **189**, 32 (2013).
[41] M. Hladík, A. Vetushka, A. Fejfar, and H. Vázquez, Phys. Chem. Chem. Phys. **21**, 6178 (2019).
[42] J. N. Hohman, S. A. Claridge, M. Kim, and P. S. Weiss, Mater. Sci. Eng.: R: Rep. **70**, 188 (2010).
[43] M. Ito, T. X. Wei, P.-L. Chen, H. Akiyama, M. Matsumoto, K. Tamada, and Y. Yamamoto, J. Mater. Chem. **15**, 478 (2005).
[44] J. C. Thomas, I. Boldog, H. S. Auluck, P. J. Bereciartua, M. Dušek, J. Macháček, Z. Bastl, P. S. Weiss, and T. Baše, Chem. Mater. **27**, 5425 (2015).
[45] D. P. Goronzy, J. Staněk, E. Avery, H. Guo, Z. Bastl, M. Dušek, N. M. Gallup, S. Gün, M. Kučeráková, B. Lewandowski, J. Macháček, V. Šícha, J. C. Thomas, A. Yavuz, K. N. Houk, M. F. Danışman, E. Mete, A. N. Alexandrova, T. Baše, and P. S. Weiss, Chem. Mater. **32**, 6800 (2020).
[46] P. Neirynck, J. Schimer, P. Jonkheijm, L.-G. Milroy, P. Cigler, and L. Brunsveld, J. Mater. Chem. B **3**, 539 (2015).
[47] H. Xiong, X. Wei, D. Zhou, Y. Qi, Z. Xie, X. Chen, X. Jing, and Y. Huang, Bioconj. Chem. **27**, 2214 (2016).
[48] H. Xiong, D. Zhou, X. Zheng, Y. Qi, Y. Wang, X. Jing, and Y. Huang, Chem. Commun. **53**, 3422 (2017).
[49] G. Kresse and D. Joubert, Phys. Rev. B **59**, 1758 (1999).
[50] P. E. Blöchl, Phys. Rev. B **50**, 17953 (1994).
[51] G. Kresse and J. Hafner, Phys. Rev. B **47**, 558 (1993).
[52] G. Kresse and J. Furthmüller, Phys. Rev. B **54**, 11169 (1996).
[53] H. Peng, Z.-H. Yang, J. P. Perdew, and J. Sun, Phys. Rev. X **6**, 041005 (2016).
[54] W. Tang, E. Sanville, and G. Henkelman, J. Phys.: Condens. Matter **21**, 084204 (2009).
[55] A. Patra, J. E. Bates, J. Sun, and J. P. Perdew, Proc. Natl. Acad. Sci. USA **114**, E9188 (2017).
[56] G. N. Derry, M. E. Kern, and E. H. Worth, J. Vac. Sci. Technol. A **33**, 060801 (2015).